Academic Journal of Science and Technology
ISSN: 2771-3032 | Vol. 14, No. 2, 2025

Study on the Characteristics of Two-phase Displacement Flow in Micro-mesh Channel of Porous Media

Dongliang Pan[1, 2], Jianqiang Sun[1, 2, *], Haizhen Zhang[3], Jing Wang[1, 2], Jie Liu[1, 2]

[1]School of Mechanical and Electrical Engineering, Southwest Petroleum University, Chengdu, Sichuan 610500, China
[2]Oil and Gas Equipment Technology Sharing and Service Platform of Sichuan Province, Chengdu 610500, China
[3]School of Science, Southwest Petroleum University, Chengdu, Sichuan 610500, China

[*]Corresponding author

Abstract: Understanding the displacement flow processes and mechanisms in porous media is fundamental for advancing oil recovery technologies. This study investigates the displacement characteristics of paraffin oil and castor oil in micro-mesh channels using CO_2 gas and distilled water as displacement media. A microfluidic experimental platform was developed to analyze phase distribution, displacement efficiency, and the interplay of interfacial tension and viscosity. Key findings include: (1) Residual oil distribution is governed by flow resistance and interfacial tension. High-resistance regions favor oil retention, while lower interfacial tension promotes dispersed residual droplets, and higher interfacial tension leads to oil accumulation in channel dead zones. (2) Displacement efficiency is influenced by viscosity contrast between oils and interfacial tension between displacement/displaced fluids. Distilled water achieves higher displacement efficiency (1.3× gas) due to stable interfacial morphology, whereas CO_2 exhibits viscous fingering effects. These results provide theoretical insights for optimizing oil recovery strategies in heterogeneous reservoirs.

Keywords: Porous media; two-phase flow; replacement; microchannel; enhance oil recovery.

1. Introduction

The exploitation of unconventional hydrocarbon reservoirs has become increasingly challenging, driving the need for advanced displacement technologies to enhance oil recovery efficiency. Concurrently, the rapid development of microfluidic techniques has positioned multiphase flow research in porous media microchannels as a prominent scientific frontier (Patel, H.V., Kuipers, J.A.M., Peters, E.: Effect of flow and fluid properties on the mobility of multiphase flows through porous media. Chemical Engineering Science 193, 243–254 (2019); Sattari, A., Hanafizadeh, P., Hoorfar, M.: Multiphase flow in microfluidics: From droplets and bubbles to the encapsulated structures. Advances in Colloid and Interface Science 282, 102208 (2020)). In reservoir systems, the intricate network of micro-nano pores within rock matrices forms complex micro-mesh channels, where the interaction between hydrocarbons and injected fluids critically determines ultimate recovery outcomes (Cai, J., Jiao, X., Wang, H., et al.: Multiphase fluid-rock interactions and flow behaviors in shale nanopores: A comprehensive review. Earth-Science Reviews 104884 (2024).; Ran, Q., Zhou, X., Ren, D., et al.: Numerical modeling of shale oil considering the influence of micro-and nanoscale pore structures. Energies 16(18), 6482 (2023)). Recent advancements span from precise multiphase fluid manipulation in microfluidic devices (Amini, Y., Ghazanfari, V., Heydari, M., et al.: Computational fluid dynamics simulation of two-phase flow patterns in a serpentine microfluidic device. Scientific Reports 13(1), 9483 (2023); Cai, J., Zhao, J., Zhong, J., et al.: Microfluidic experiments and numerical simulation methods of pore-scale multiphase flow. Capillarity 12(1), 1–5 (2024)) to innovative strategies for enhanced oil recovery (You, Q., Wen, Q., Fang, J., et al.: Experimental study on lateral flooding for enhanced oil recovery in bottom-water reservoir with high water cut. Journal of Petroleum Science and Engineering 174, 747–756 (2019); Fani, M., Pourafshary, P., Mostaghimi, P., et al.: Application of microfluidics in chemical enhanced oil recovery: A review. Fuel 315, 123225 (2022)), underscoring the necessity to investigate displacement dynamics across diverse porous media and oil types (Li, X., Xiao, K., Wang, R., et al.: Experimental research on enhanced oil recovery methods for gas injection of fractured reservoirs based on microfluidic chips. ACS Omega 7(31), 27382–27389 (2022); Seyyedi, M., Sohrabi, M.: Oil reservoir on a chip: Pore-scale study of multiphase flow during near-miscible CO_2 EOR and storage. Transport in Porous Media 134(2), 331–349 (2020)).

The viscosity and chemical composition of oils significantly influence displacement behavior and residual oil distribution. Systematic analysis of these interactions in micro-mesh channels enables optimization of displacement media selection for specific reservoir conditions. Among displacement agents, CO_2 gas and water emerge as representative candidates due to their distinct mechanisms(He, L., Jiaping, T., Siwei, M., et al.: Application and prospects of CO2 enhanced oil recovery technology in shale oil reservoir. China Petroleum Exploration 27(1), 127 (2022); Wang, H., Su, Y., Wang, W., et al.: CO_2-oil diffusion, adsorption and miscible flow in nanoporous media from pore-scale perspectives. Chemical Engineering Journal 450, 137957 (2022); Foroozesh, J., Kumar, S.: Nanoparticles behaviors in porous media: Application to enhanced oil recovery. Journal of Molecular Liquids 316, 113876 (2020); Wang, L., Zhang, Y., Zou, R., et al.: Dynamics of oil–CO_2–water three-phase under the nanopore confinement effect: Implications for CO_2 enhanced shale oil recovery and carbon storage. Separation and Purification Technology 354, 128892

(2025); Song, Z., Li, Y., Song, Y., et al.: A critical review of CO_2 enhanced oil recovery in tight oil reservoirs of North America and China. SPE Asia Pacific Oil and Gas Conference and Exhibition, SPE-2020-APOGCE-D011S005R002 (2020)): CO_2 injection enhances recovery through viscosity reduction, light-component extraction, and miscibility with crude oil (Kumar, N., Sampaio, M.A., Ojha, K., et al.: Fundamental aspects, mechanisms and emerging possibilities of CO_2 miscible flooding in enhanced oil recovery: A review. Fuel 330, 125633 (2022); Zhang, Z., Bai, M., Xu, L., et al.: Study on oil extraction characteristics in micropores of a typical terrestrial shale reservoir in China by CO_2 injection and surfactant imbibition. Energy & Fuels 38(8), 6927–6937 (2024); Zuo, M., Chen, H., Qi, X., et al.: Effects of CO_2 injection volume and formation of in-situ new phase on oil phase behavior during CO_2 injection for enhanced oil recovery (EOR) in tight oil reservoirs. Chemical Engineering Journal 452, 139454 (2023); Zhang, X., Li, L., Su, Y., et al.: Microfluidic investigation on asphaltene interfaces attempts to carbon sequestration and leakage: Oil-CO_2 phase interaction characteristics at ultrahigh temperature and pressure. Applied Energy 348, 121518 (2023); Li, L., Kang, Y., Liu, F., et al.: Experimental study on the mass transfer and microscopic distribution characteristics of remaining oil and CO_2 during water-miscible CO_2 flooding. Journal of CO_2 Utilization 87, 102920 (2024)) while water flooding leverages wettability alteration and interfacial stability (Xiangguo, L.U., Bao, C.A.O., Kun, X.I.E., et al.: Enhanced oil recovery mechanisms of polymer flooding in a heterogeneous oil reservoir. Petroleum Exploration and Development 48(1), 169–178 (2021); Liu, F., Wang, M.: Review of low salinity waterflooding mechanisms: Wettability alteration and its impact on oil recovery. Fuel 267, 117112 (2020); Wang, J., Song, H., Wang, Y.: Investigation on the micro-flow mechanism of enhanced oil recovery by low-salinity water flooding in carbonate reservoir. Fuel 266, 117156 (2020)). Notably, CO_2 demonstrates low interfacial tension with oils, facilitating phase dispersion and residual saturation reduction in low-viscosity systems under high-pressure conditions . In contrast, water's higher density and interfacial tension enable stable displacement fronts(Lu, M., Qian, Q., Zhong, A., et al.: Investigation on the flow behavior and mechanisms of water flooding and CO_2 immiscible/miscible flooding in shale oil reservoirs. Journal of CO2 Utilization 80, 102660 (2024)), though concomitant water film formation may impede flow in high-viscosity scenarios (Arab, D., Kantzas, A., Bryant, S.L.: Water flooding of oil reservoirs: Effect of oil viscosity and injection velocity on the interplay between capillary and viscous forces. Journal of Petroleum Science and Engineering 186, 106691 (2020)).

Despite these advancements, comparative studies on CO_2 and water displacement efficiencies under controlled flow rates remain limited, particularly regarding residual oil distribution in geometrically constrained micro-mesh channels. Existing research gaps include: (1) insufficient understanding of how viscosity contrasts and interfacial tension govern displacement patterns; (2) lack of systematic analysis of viscous fingering effects in CO_2 flooding; and (3) limited integration of microscale experimental data with reservoir-scale recovery strategies. Addressing these challenges requires advanced microfluidic platforms capable of resolving phase evolution and pressure dynamics at pore-scale resolutions (Burrows, L.C., Haeri, F., Cvetic, P., et al.: A literature review of CO2, natural gas, and water-based fluids for enhanced oil recovery in unconventional reservoirs. Energy & Fuels 34(5), 5331–5380 (2020); Mehdi Sattari-Najafabadi, Mohsen Nasr Esfahany, Zan Wu, Bengt Sunden.: Mass transfer between phases in microchannels: A review. Chemical Engineering and Processing - Process Intensification 127, 213–237 (2018)).

Motivated by these needs, this study employs a customized microfluidic chip to investigate CO_2 and water displacement behaviors for paraffin oil (low viscosity) and castor oil (high viscosity) under fixed flow rates. By combining high-speed visualization with numerical simulations, we quantify the roles of interfacial tension, viscosity contrast, and channel resistance in determining displacement efficiency and residual oil morphology. Our findings provide critical insights for optimizing displacement media selection and operational parameters in heterogeneous reservoirs.

2. Experimental Design

A polydimethylsiloxane (PDMS) microfluidic chip was fabricated with a mesh-structured channel (width: 0.2 mm, depth: 0.1 mm) using photolithography (Fig. 1a). The fluidic system comprised three phases: distilled water (dyed with methyl blue), paraffin oil, and castor oil (stained with Sudan III for enhanced visualization).

The experimental setup (Fig. 1b) included: A high-speed camera (Phantom VEO 640L, VEO, USA) with a resolution of 1920 × 1080 pixels and a sampling rate of 24 frames/s (exposure time: 0.416 s/frame).A precision syringe pump (5 mL syringe, inner diameter: 13 mm, outer diameter: 14 mm) connected to the channel inlet via a 0.5 mm needle and PTFE tubing (length: 64 mm).A backlight illumination system to ensure uniform contrast for flow visualization. The chip was securely mounted on an anti-vibration stage to minimize external perturbations. Fluid flow was regulated at 0.5 mL/min, enabling real-time monitoring of displacement dynamics. The outlet remained open to atmospheric pressure, while the entire system was maintained at 25°C (±0.5°C) to ensure experimental consistency.

The thermophysical properties of three experimental fluids (distilled water, paraffin oil, and castor oil) were systematically characterized at 25°C using standardized measurement protocols, with key parameters including density, dynamic viscosity, and surface tension summarized in Table 1. A comparative displacement study was conducted through three experimental configurations: (1) CO_2 gas displacing paraffin oil and castor oil, (2) distilled water displacing paraffin oil and castor oil, (3) CO_2 gas displacing distilled water as the control group. The displacement dynamics were quantitatively analyzed through real-time monitoring of interfacial phenomena and subsequent calculation of displacement efficiency. Experimental observations revealed that a controlled injection rate of 0.5 mL/min optimized the visualization of displacement characteristics, particularly in terms of interface stability and fluid fingering patterns. This optimized flow condition facilitated comprehensive analysis of multiphase flow behavior, including capillary number effects and viscosity-dominated displacement mechanisms.

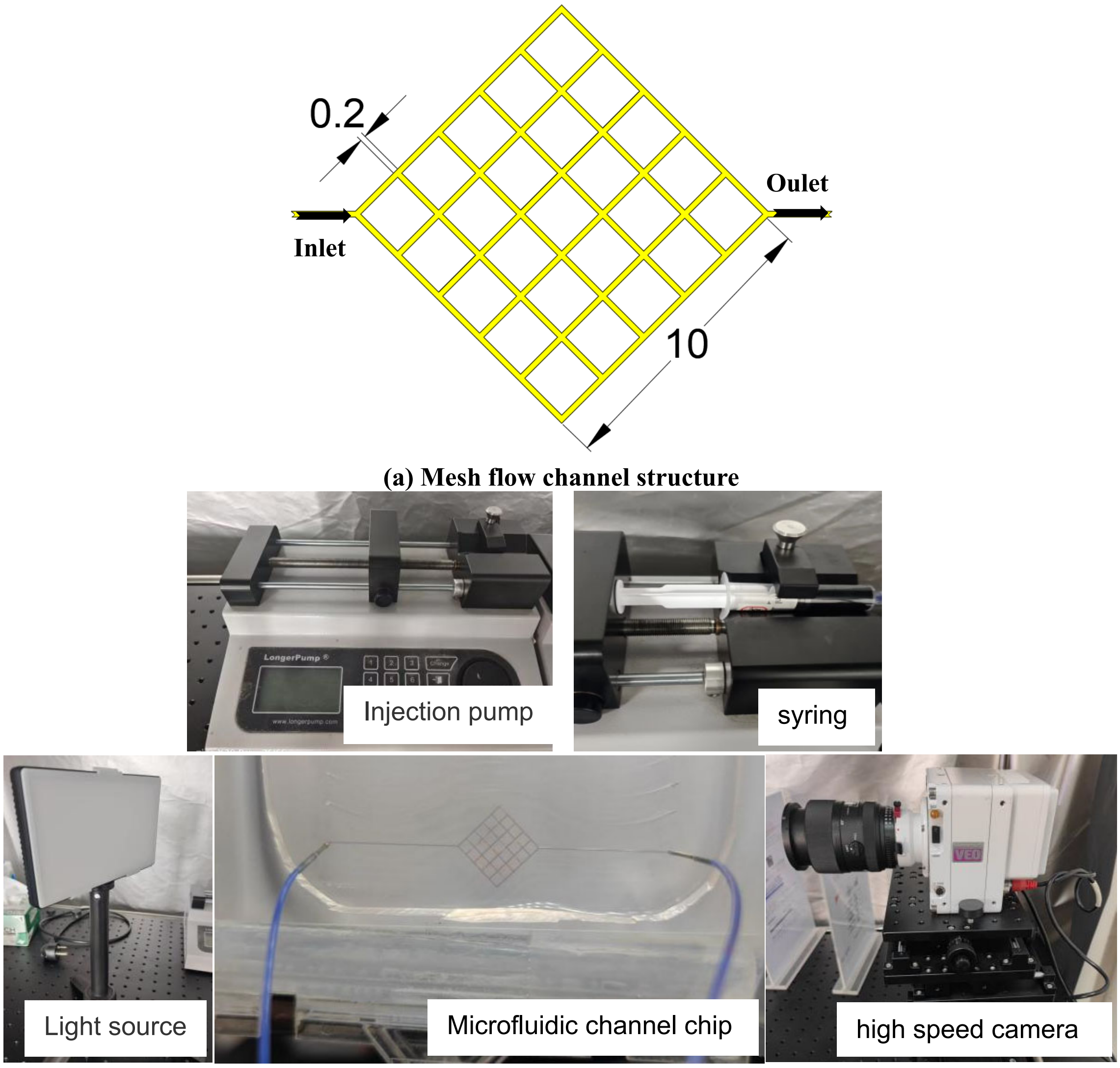

(a) Mesh flow channel structure

(b) Experimental device

Figure 1. Mesh channel and experimental device

Table 1. Fluid physical parameters

Fluid type	Distilled water	Paraffin oil	Castor oil
Viscosity / mPa·s	0.894	36	612
Density / g/cm^3	1	0.8	0.96
surface tension / mN/m	72.8	27.5	36.1

3. Results and Discussion

3.1. Analysis of displacement process

The dynamic evolution of phase distributions (oil, water, CO_2 gas) during the displacement process in micromesh channels was captured using high-speed imaging. In the initial stage of displacement, the oil phase predominantly occupied the channel volume. As CO_2 flooding progressed, CO_2 preferentially migrated into the central flow region, displacing the oil phase toward channel peripheries and trapping it in dead-end pores within multibend segments (Fig. 2). The residual oil phase (black) and advancing CO_2 gas phase (white) illustrate this immiscible displacement mechanism.

In contrast, water flooding exhibited distinct behavior due to oil-water immiscibility. A sharp oil-water interface formed within the channel, with water preferentially wetting the walls to generate a continuous aqueous film. This wettability-driven process resulted in residual oil films adhering to the channel surfaces (Fig. 3). For water flooding experiments (Fig. 3), the injected water phase appears black, while the displaced air at the channel inlet is visualized as white. The transparent phase corresponds to residual oil retained in pore networks, demonstrating incomplete displacement efficiency under immiscible conditions. These observations align with wettability and interfacial dynamics described by Mahmoudzadeh et al. (Mahmoudzadeh, A., Fatemi, M., Masihi, M.: Microfluidics experimental investigation of the mechanisms of enhanced oil recovery by low salinity water flooding in fractured porous media. Fuel 314, 123067 (2022)).

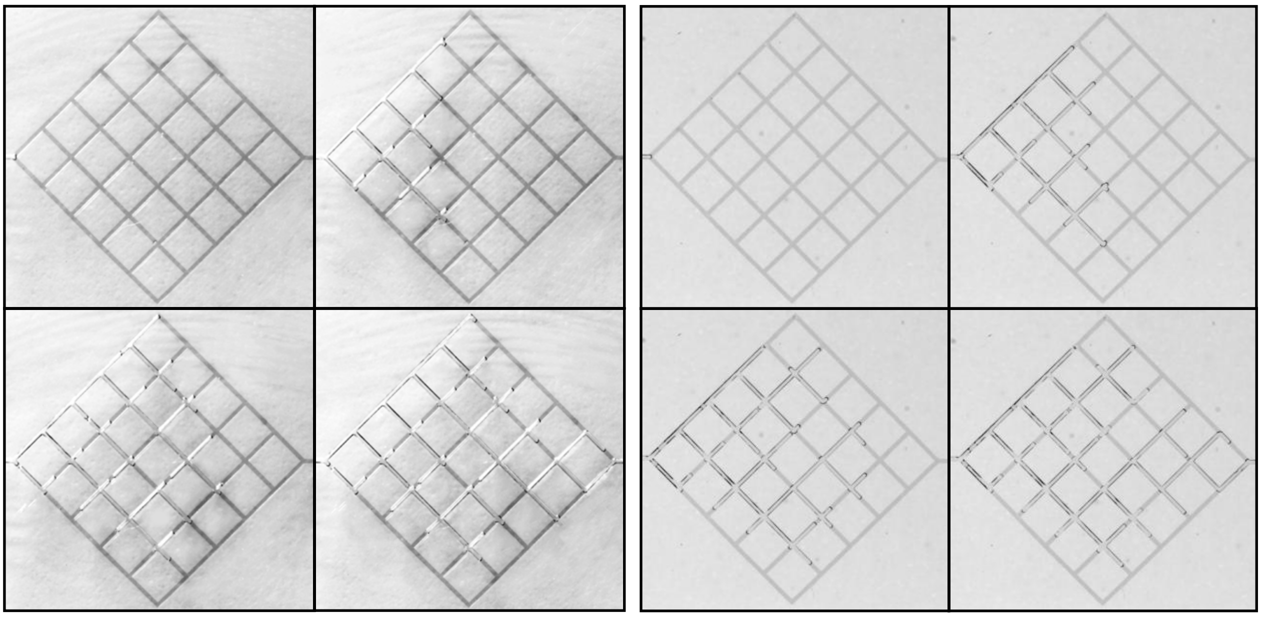

(a) CO_2 gas displacement Paraffin Oil **(b) CO_2 gas displacement castor oil**

Figure 2. CO_2 gas displacement process

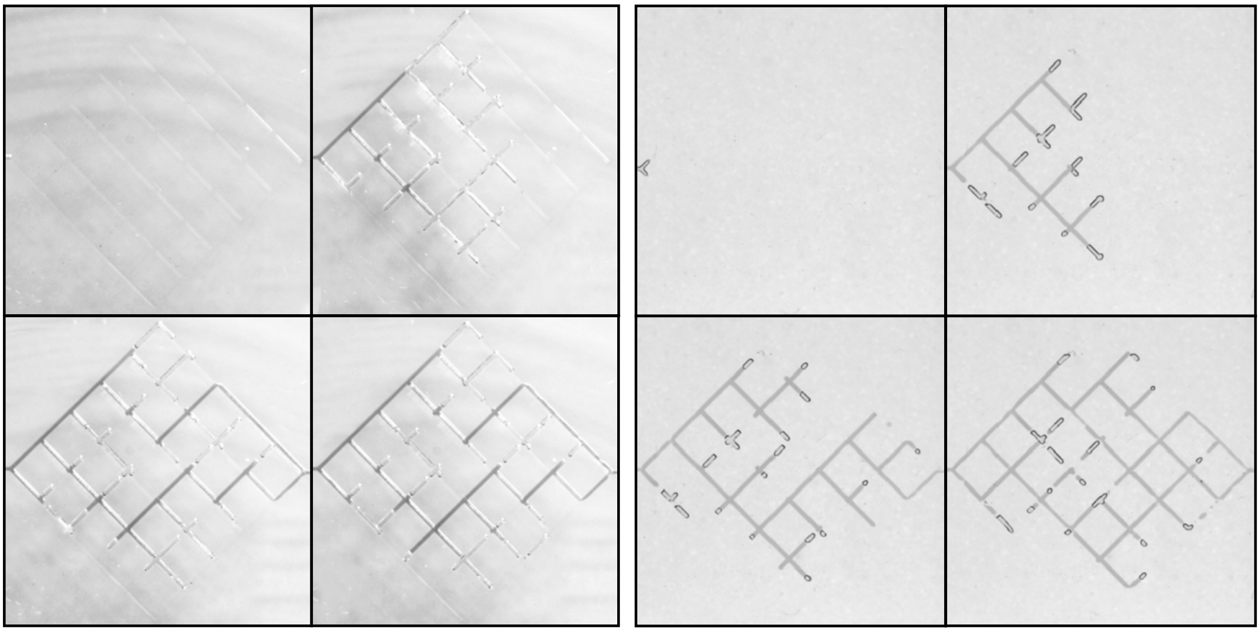

(a) Distilled water displacement paraffin oil **(b) Distilled water displacement castor oil**

Figure 3. Distilled water displacement process

Displacement efficiency: displacement efficiency = (initial oil volume − remaining oil volume) / initial oil volume × 100 %

The temporal evolution of displacement processes was quantified through systematic measurement of interfacial stabilization times, defined as the duration from initial fluid invasion to final stabilization of fluid interfaces. Experimental results revealed significant variations in displacement kinetics across different fluid pairs: (1) CO_2 gas displacement of paraffin oil demonstrated a mean displacement duration of 4.17 s, (2) water-castor oil systems required 38.62 s for complete interfacial equilibration (the longest observed stabilization period), while (3) water-paraffin oil and water-castor oil combinations exhibited shorter stabilization times of 2.87 s and 3.75 s, respectively. These temporal disparities primarily stemmed from viscosity contrasts between displacing/displaced fluids and interfacial tension characteristics.

Quantitative analysis of displacement efficiency dynamics was performed through digital image analysis using Image J, with normalized temporal progression (horizontal axis) representing the ratio of elapsed time to total displacement duration, and instantaneous displacement efficiency (vertical axis) calculated as the proportion of displaced volume relative to total pore volume. The resultant efficiency-time profiles (Fig. 4) demonstrate characteristic sigmoidal patterns, with nonlinear regression analysis revealing distinct inflection points corresponding to breakthrough events. Notably, the CO_2-paraffin oil system exhibited 92% efficiency attainment within the first 40% of normalized time, contrasting with the water-castor oil system's gradual efficiency increase (68% efficiency at equivalent normalized time). These differential behaviors underscore the dominant influence of viscosity ratio (M) and capillary number (Ca) on displacement front propagation dynamics.

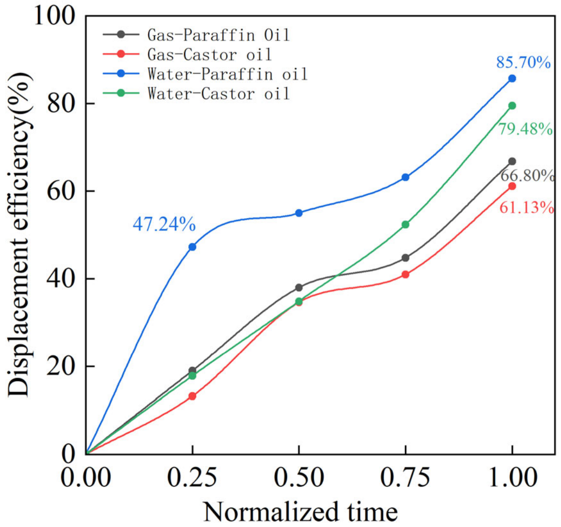

Figure 4. The displacement efficiency of different media varies with time.

This investigation systematically evaluates the displacement kinetics of paraffinic and castor oils under two distinct displacement media (CO_2 gas and distilled water) through temporal evolution analysis. Key displacement parameters including rate dynamics, efficiency evolution, and stabilization characteristics were quantitatively compared (Figure 4).

CO_2-Paraffin Oil System (Black curve)

The CO_2-paraffin oil system demonstrated rapid displacement kinetics with stabilization achieved within 4.17 s, reaching 66.8% final displacement efficiency. This enhanced performance originates from favorable interfacial interactions - the low interfacial tension between CO_2 and paraffin oil ($\sigma = 6.5$ mN/m) coupled with the Newtonian fluid characteristics of low-viscosity paraffin oil facilitated uniform displacement front propagation. Notably, 90% of maximum efficiency was attained within the initial 2.1 s, indicating pseudolinear displacement behavior.

CO_2-Castor Oil System (Red curve)

High-viscosity castor oil exhibited significant flow resistance under CO2 displacement, extending the stabilization time to 38.62 s - an order-of-magnitude increase compared to paraffin oil. The efficiency profile showed gradual monotonic growth (0-61.13%) with characteristic logarithmic time dependence (R^2=0.98). This pronounced viscous dominance suggests shear-thinning behavior where displacement rate inversely correlates with instantaneous viscosity ($\partial v/\partial \mu = -k$).

Distilled water-Paraffin Oil System (Blue curve)

Distilled water achieved superior displacement performance with 85.7% final efficiency in merely 2.87 s. The biphasic displacement profile revealed: (a) An initial rapid phase (0-0.72 s) achieving 47.24% efficiency through capillary-dominated flow, and (b) A subsequent film drainage-controlled regime where efficiency asymptotically approached maximum values. This transition corresponds to the critical capillary number ($Ca=1\times10^{-3}$) where viscous forces overcome interfacial effects.

Distilled water-Castor oil System (Green curve)

The water-castor oil system displayed unique displacement characteristics with prolonged stabilization time (3.75 s) and 79.48% final efficiency. Comparative analysis showed 23% slower initial displacement rate than CO_2-paraffin system, attributable to competing effects of aqueous phase fingering and oil phase elastic recovery. The stable efficiency plateau suggests achieved mechanical equilibrium between displacement and capillary retention forces.

Mechanistic Interpretation.

The temporal displacement patterns fundamentally depend on the viscosity ratio ($M = \mu d/\mu o$) and capillary number (Ca). Water systems ($M < 1$) generally exhibited higher Ca values (10^{-2}-10^{-3}) compared to gas systems ($Ca \sim 10^{-4}$), explaining their superior efficiency through improved viscous coupling. However, gas displacement showed unique advantages in low-viscosity systems through enhanced interfacial mass transfer and solubility effects.

This comprehensive analysis provides quantitative benchmarks for predicting displacement behavior in porous media applications, particularly relevant to enhanced oil recovery and subsurface carbon sequestration strategies. The time-dependent efficiency models developed here enable better optimization of injection parameters based on fluid rheological properties.

3.2. Residual Oil Distribution

Principle of Hydraulic Priority Pathway Selection in Porous Media.

Fluid migration through porous media adheres to the energy minimization principle (Nimmo, J.R.: The processes of preferential flow in the unsaturated zone. Soil Science Society of America Journal 85(1), 1–27 (2021)), wherein fluids tend to preferentially migrate through pathways characterized by lower hydraulic resistance to minimize energy expenditure. This selective flow behavior results in capillary-driven displacement processes favoring low-resistance conduits, while high-resistance pathways with acute bending angles or irregular wall morphology induce capillary trapping of the oil phase due to insufficient driving potential. A positive correlation exists between conduit length and cumulative flow resistance, as described by the Hagen-Poiseuille relationship. Consequently, residual oil saturation predominantly occurs along the upper and lower walls within the distal segment of the flow channel (Figure 5a).

Furthermore, localized hydraulic losses significantly influence residual oil distribution in reticulated pore networks. Numerical simulations of oil-phase transport through a central tortuous channel (comprising one inlet-outlet pair, two 45° bends, and eight 90° bends) reveal maximized frictional losses under such geometric constraints (Ke, W., Liu, Y., Zhao, X., et al.: Study on the effect of threshold pressure gradient on remaining oil distribution in heavy oil reservoirs. ACS Omega 7(5), 3949–3962 (2022)). As illustrated in Figure 5b, the peak localized hydraulic loss h_j attains 3.904×10^-3 m. These high-energy dissipation zones correspond to preferential sites for oil-phase retention, demonstrating a direct relationship between flow path tortuosity and residual hydrocarbon accumulation.

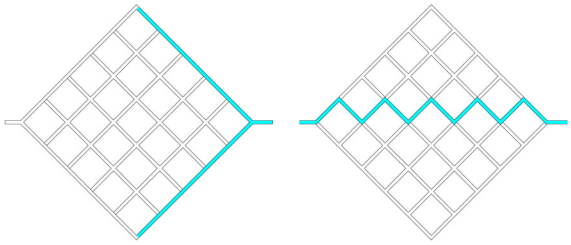

(a) Large resistance along the way **(b) Large local resistance**

Figure 5. Analysis of residual oil distribution position

Figure 6 illustrates the residual liquid distribution following CO_2 gas displacement. The high mobility of CO_2 in mesoscale channels induces preferential infiltration into pathways with lower capillary resistance, establishing stable flow paths that lead to non-uniform displacement efficiency and complex interfacial configurations characterized by pronounced fingering effects.

In the paraffin oil displacement (Fig. 6a), continuous residual oil accumulation at the channel base demonstrates the synergistic action of gravitational segregation and viscous fingering. Post-stabilization, mobilized droplets undergo wall-directed migration, culminating in basal coalescence. Secondary residual oil distributions appear as discrete droplets in mid-channel tortuous regions and upper posterior sections. Comparative analysis of castor oil displacement (Fig. 6b) reveals reduced basal continuity relative to paraffin oil. The elevated viscosity of castor oil promotes wall-adherent film formation through enhanced viscous dominance over gravitational effects. CO2's low interfacial tension exacerbates wall wettability sensitivity and flow instability, inducing dynamic film fragmentation mechanisms. Visual tracking captured sequential oil phase transformations from continuous films to filamentary structures and ultimately discrete droplets prior to expulsion.

Figure 7 presents aqueous displacement characteristics using distilled water, where high interfacial tension and favorable wettability promote stable frontal advancement with minimized fingering. The aqueous phase forms wall-adherent films that progressively constrict oil phases toward pore centroids.

Paraffin oil displacement by Distilled water (Fig. 7a) shows marked efficiency improvement over gaseous displacement, with residual oil localized in mid-channel and posterior regions. Castor oil displacement (Fig. 7b) exhibits exceptional clearance efficiency, with residual oil accumulating in upper/lower corner menisci. An anomalous lower-left accumulation suggests early-stage flow path establishment where aqueous phase preferential channeling creates insufficient driving potential for complete oil mobilization. In situ observations revealed oil droplet fragmentation and aqueous-mediated transport, generating oil-water emulsions at outflow regions.

Numerical simulations in Figures 8 (CO_2 displacement) and 9 (Distilled water displacement) demonstrate strong congruence with experimental results, accurately predicting residual oil localization in high-resistance tortuous mid-sections and posterior wall regions. The models successfully capture the dual influence of gravitational and capillary forces on final saturation distributions.

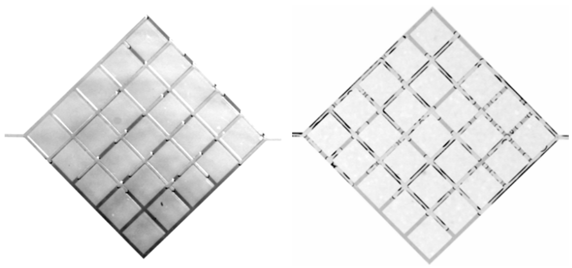

(a) CO_2 gas displacement Paraffin Oil **(b) CO_2 gas displacement castor oil**

Figure 6. Residue of CO_2 gas replacing liquid phase

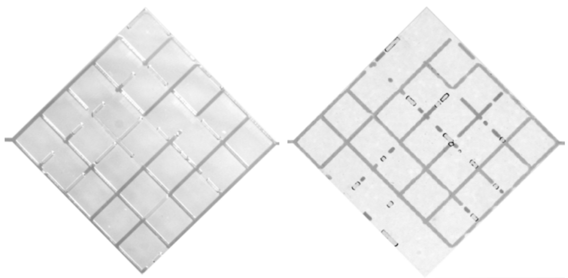

(a) Distilled water displacement paraffin oil **(b) Distilled water displacement castor oil**

Figure 7. Residue of oil phase replaced by distilled water

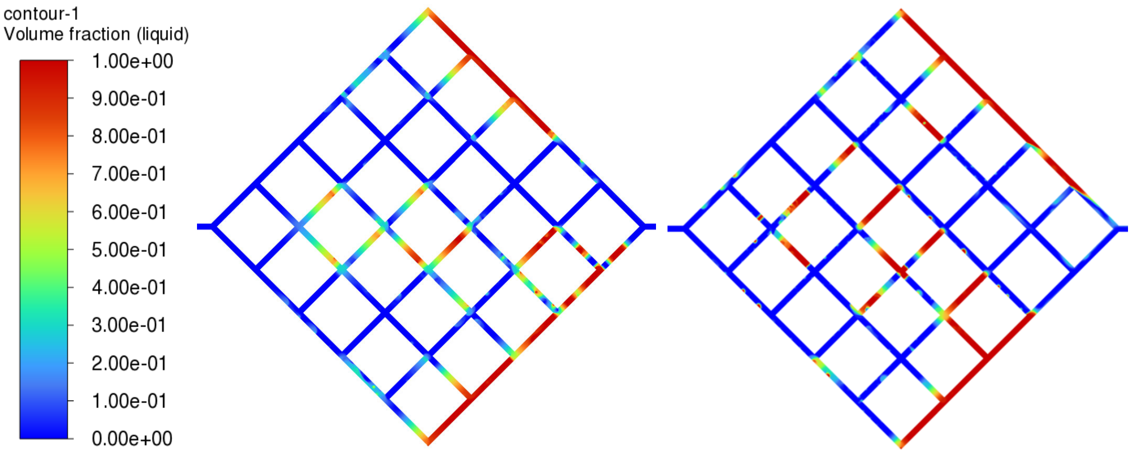

(a) CO_2 gas displacement Paraffin Oil **(b) CO_2 gas displacement castor oil**

Figure 8. Simulation of oil phase residue by CO_2 gas displacement

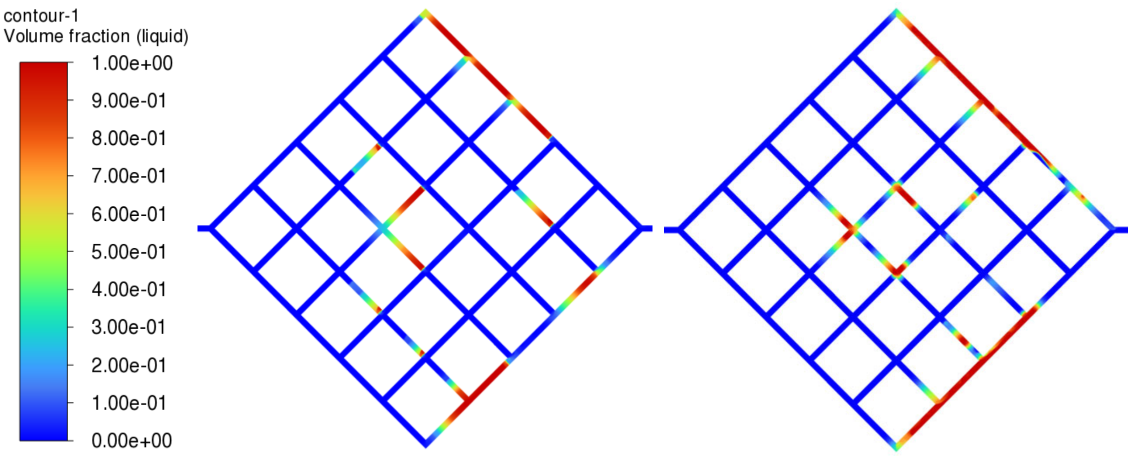

(a) Distilled water displacement paraffin oil **(b) Distilled water displacement castor oil**

Figure 9. Distilled water substitutes for simulated oil phase residue

3.3. Key Influencing Factors

The final displacement efficiency is shown in Fig. 10. The efficiency of CO_2 displacing paraffin oil is 66.8 %, which is about 5.67 % higher than that of displacing castor oil (61.13 %). The efficiency of displacement of paraffin oil by distilled water is 85.7 %, which is about 6.22 % higher than that of displacement of castor oil. The displacement efficiency of CO_2 displacing distilled water in the control group was 75.89 %.

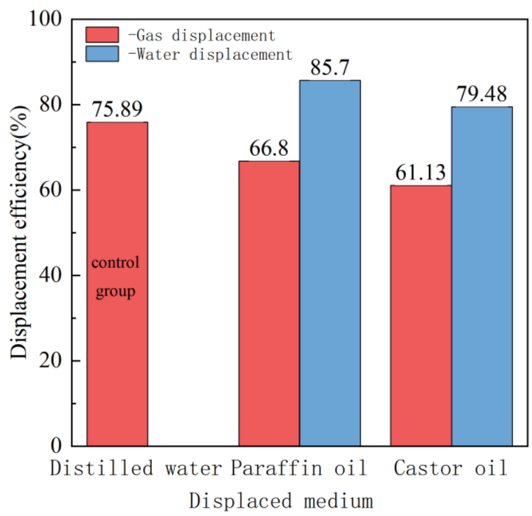

Figure 10. Final displacement efficiency

At 25 °C standard atmosphere, the interfacial tension between CO_2 and paraffin oil is 6.5 mN/m, and the interfacial tension between CO_2 and castor oil is 4.8 mN/m, which is a low interfacial tension displacement medium. The interfacial tension between distilled water and paraffin oil is 28.1 mN/m, and the interfacial tension between distilled water and castor oil is 32.4 mN/m, which belongs to the displacement medium with high interfacial tension.

(1) Effect of Viscosity

Because the chemical structure and physical properties of paraffin oil are different from those of castor oil, their interaction with CO_2 is also different. The viscosity of paraffin oil is low, and the displacement medium can more easily promote the flow of paraffin oil in the channel, thereby improving the displacement efficiency. The viscosity of castor oil is higher, and the viscous resistance increases significantly, which leads to the need to overcome greater resistance of the displacement medium, and the displacement efficiency is limited. In the final state, the displacement efficiency of CO_2 to castor oil is lower than that of paraffin oil. This is because the higher viscosity of castor oil and more polar groups in its molecular structure make it more difficult for carbon dioxide to dissolve into it and change its fluidity. In the control group, although distilled water and CO_2 have a high interfacial tension, the extremely low viscosity makes the displacement efficiency the highest. For the displacement of castor oil, due to its high viscosity characteristics, whether it is CO_2 or distilled water, it shows a certain displacement efficiency limit. Viscous resistance aggravates the instability of interface morphology and makes the displacement efficiency low. Therefore, the viscosity of the displaced fluid is one of the important factors affecting the displacement efficiency.

(2) Effect of interfacial tension

Lower interfacial tension will lead to enhanced interfacial stability, which can form a more stable interface morphology, thereby improving the displacement efficiency. Under the same experimental conditions, in order to eliminate the influence of viscosity, the interfacial tension between CO_2 and paraffin oil is larger than that between CO_2 and castor oil, and the interfacial tension between distilled water and paraffin oil is smaller than that between distilled water and castor oil. In the displacement results, the efficiency of displacement of paraffin oil by distilled water is 6.22 % higher than that of displacement of castor oil, and the efficiency of displacement of paraffin oil by CO_2 is only 5.67 % higher than that of displacement of castor oil, which is less than 6.22 % of displacement of distilled water. Therefore, the influence of interfacial tension on displacement efficiency can also be reflected.

(3) Effect of viscous fingering

The intermiscibility of CO_2 and oil is good, and finger-like diffusion will be formed on the interface, which is called fingering effect. The fingering effect will cause the displacement medium to be unable to evenly promote the oil layer, and the oil in some areas will be wrapped or residual, which will significantly reduce the final displacement efficiency. In the control group, the efficiency of CO_2 flooding distilled water was 9.09 % and 14.76 % higher than that of flooding paraffin oil and castor oil, respectively. This is because the wettability of water weakens the fingering effect, thus improving the displacement efficiency.

4. Conclusions

In this paper, a microfluidic experimental platform was built to explore the residual oil phase distribution characteristics of CO_2 gas and distilled water displacing the non-oil phase and the influencing factors of displacement efficiency. The main results are as follows :

The resistance along the way and the local resistance determine the distribution position of the residual oil, and the interfacial tension determines the distribution pattern of the residual oil after the experiment. Where the resistance is large, the oil phase is easy to remain. The lower interfacial tension will cause the oil droplets to form a small and dispersed residue in the channel, and the higher interfacial tension makes the residual oil accumulate at the dead angle or mesh node of the channel in a larger volume.

The influencing factors of displacement efficiency are the viscosity difference between paraffin oil and castor oil and the interfacial tension between the displacement medium and the displaced medium. In addition, the fingering effect in the displacement process will also affect the final displacement efficiency. As a high viscosity displaced medium, the overall displacement efficiency of castor oil is lower than that of paraffin oil. The viscosity of paraffin oil is low, and the displacement efficiency is relatively high. The viscosity of castor oil is higher, which increases the resistance in the displacement process and significantly limits the permeability and driving ability of the displacement medium. The displacement rate of the two displacement media decreased. The lower interfacial tension can weaken the capillary force and enhance the viscous force, which is beneficial to the separation of oil-water interface and the displacement of oil phase. Distilled water as the displacement medium, the overall efficiency is better than CO_2. The fingering effect of CO_2 leads to the failure of oil in some areas to obtain sufficient driving force and cannot be completely displaced, which reduces the final displacement efficiency. The distilled water displacement process can form a stable interface morphology, and a higher driving pressure can be obtained in the mesh channel to promote the overall movement of the oil layer, thereby improving the displacement efficiency.

Comprehensive analysis shows that CO_2 is more suitable for the displacement of low viscosity oil. When CO_2 is dissolved in crude oil, the volume of crude oil will expand and the viscosity will decrease, which is conducive to the displacement of CO_2. In the CO_2 displacement to enhance oil recovery, the pressure of displacement can be increased and the fingering effect can be weakened to increase the displacement efficiency. Similarly, supercritical CO_2 can also be used to further reduce the interfacial tension and weaken the fingering phenomenon to optimize the displacement effect. In the actual displacement to improve oil recovery, the displacement efficiency can also be improved by reducing the interfacial tension. For example, in the water flooding enhanced oil recovery technology, adding surfactants to distilled water reduces the interfacial tension between water and oil, making it easier for water to penetrate the oil layer and increasing the oil displacement rate. Future research will further explore the effects of different surfactants on the displacement efficiency of distilled water and CO_2, explore how to reduce the viscosity of crude oil to improve oil recovery, and the displacement law under more complex porous media models and actual formation conditions.

References

[1] Amini, Y., Ghazanfari, V., Heydari, M., et al.: Computational fluid dynamics simulation of two-phase flow patterns in a serpentine microfluidic device. Scientific Reports 13(1), 9483 (2023)

[2] Arab, D., Kantzas, A., Bryant, S.L.: Water flooding of oil reservoirs: Effect of oil viscosity and injection velocity on the interplay between capillary and viscous forces. Journal of Petroleum Science and Engineering 186, 106691 (2020)

[3] Burrows, L.C., Haeri, F., Cvetic, P., et al.: A literature review of CO2, natural gas, and water-based fluids for enhanced oil recovery in unconventional reservoirs. Energy & Fuels 34(5), 5331–5380 (2020)

[4] Cai, J., Jiao, X., Wang, H., et al.: Multiphase fluid-rock interactions and flow behaviors in shale nanopores: A comprehensive review. Earth-Science Reviews 104884 (2024).

[5] Cai, J., Zhao, J., Zhong, J., et al.: Microfluidic experiments and numerical simulation methods of pore-scale multiphase flow. Capillarity 12(1), 1–5 (2024)

[6] Fani, M., Pourafshary, P., Mostaghimi, P., et al.: Application of microfluidics in chemical enhanced oil recovery: A review. Fuel 315, 123225 (2022)

[7] Foroozesh, J., Kumar, S.: Nanoparticles behaviors in porous media: Application to enhanced oil recovery. Journal of Molecular Liquids 316, 113876 (2020)

[8] He, L., Jiaping, T., Siwei, M., et al.: Application and prospects of CO2 enhanced oil recovery technology in shale oil reservoir. China Petroleum Exploration 27(1), 127 (2022)

[9] Ke, W., Liu, Y., Zhao, X., et al.: Study on the effect of threshold pressure gradient on remaining oil distribution in heavy oil reservoirs. ACS Omega 7(5), 3949–3962 (2022)

[10] Kumar, N., Sampaio, M.A., Ojha, K., et al.: Fundamental aspects, mechanisms and emerging possibilities of CO_2 miscible flooding in enhanced oil recovery: A review. Fuel 330, 125633 (2022)

[11] Li, L., Kang, Y., Liu, F., et al.: Experimental study on the mass transfer and microscopic distribution characteristics of remaining oil and CO_2 during water-miscible CO_2 flooding. Journal of CO_2 Utilization 87, 102920 (2024)

[12] Li, X., Xiao, K., Wang, R., et al.: Experimental research on enhanced oil recovery methods for gas injection of fractured reservoirs based on microfluidic chips. ACS Omega 7(31), 27382–27389 (2022)

[13] Liu, F., Wang, M.: Review of low salinity waterflooding mechanisms: Wettability alteration and its impact on oil recovery. Fuel 267, 117112 (2020)

[14] Lu, M., Qian, Q., Zhong, A., et al.: Investigation on the flow behavior and mechanisms of water flooding and CO_2 immiscible/miscible flooding in shale oil reservoirs. Journal of CO2 Utilization 80, 102660 (2024)

[15] Mahmoudzadeh, A., Fatemi, M., Masihi, M.: Microfluidics experimental investigation of the mechanisms of enhanced oil recovery by low salinity water flooding in fractured porous media. Fuel 314, 123067 (2022)

[16] Mehdi Sattari-Najafabadi, Mohsen Nasr Esfahany, Zan Wu, Bengt Sunden.: Mass transfer between phases in microchannels: A review. Chemical Engineering and Processing - Process Intensification 127, 213–237 (2018)

[17] Nimmo, J.R.: The processes of preferential flow in the unsaturated zone. Soil Science Society of America Journal 85(1), 1–27 (2021)

[18] Patel, H.V., Kuipers, J.A.M., Peters, E.: Effect of flow and fluid properties on the mobility of multiphase flows through porous media. Chemical Engineering Science 193, 243–254 (2019)

[19] Ran, Q., Zhou, X., Ren, D., et al.: Numerical modeling of shale oil considering the influence of micro-and nanoscale pore structures. Energies 16(18), 6482 (2023)

[20] Sattari, A., Hanafizadeh, P., Hoorfar, M.: Multiphase flow in microfluidics: From droplets and bubbles to the encapsulated structures. Advances in Colloid and Interface Science 282, 102208 (2020)

[21] Seyyedi, M., Sohrabi, M.: Oil reservoir on a chip: Pore-scale study of multiphase flow during near-miscible CO_2 EOR and storage. Transport in Porous Media 134(2), 331–349 (2020)

[22] Song, Z., Li, Y., Song, Y., et al.: A critical review of CO_2 enhanced oil recovery in tight oil reservoirs of North America and China. SPE Asia Pacific Oil and Gas Conference and Exhibition, SPE-2020-APOGCE-D011S005R002 (2020)

[23] Wang, H., Su, Y., Wang, W., et al.: CO_2-oil diffusion, adsorption and miscible flow in nanoporous media from pore-scale perspectives. Chemical Engineering Journal 450, 137957 (2022)

[24] Wang, J., Song, H., Wang, Y.: Investigation on the micro-flow mechanism of enhanced oil recovery by low-salinity water flooding in carbonate reservoir. Fuel 266, 117156 (2020)

[25] Wang, L., Zhang, Y., Zou, R., et al.: Dynamics of oil–CO_2–water three-phase under the nanopore confinement effect: Implications for CO_2 enhanced shale oil recovery and carbon storage. Separation and Purification Technology 354, 128892 (2025)

[26] Xiangguo, L.U., Bao, C.A.O., Kun, X.I.E., et al.: Enhanced oil recovery mechanisms of polymer flooding in a heterogeneous oil reservoir. Petroleum Exploration and Development 48(1), 169–178 (2021)

[27] You, Q., Wen, Q., Fang, J., et al.: Experimental study on lateral flooding for enhanced oil recovery in bottom-water reservoir with high water cut. Journal of Petroleum Science and Engineering 174, 747–756 (2019)

[28] Zhang, X., Li, L., Su, Y., et al.: Microfluidic investigation on asphaltene interfaces attempts to carbon sequestration and leakage: Oil-CO_2 phase interaction characteristics at ultrahigh temperature and pressure. Applied Energy 348, 121518 (2023)

[29] Zhang, Z., Bai, M., Xu, L., et al.: Study on oil extraction characteristics in micropores of a typical terrestrial shale reservoir in China by CO_2 injection and surfactant imbibition. Energy & Fuels 38(8), 6927–6937 (2024)

[30] Zuo, M., Chen, H., Qi, X., et al.: Effects of CO_2 injection volume and formation of in-situ new phase on oil phase behavior during CO_2 injection for enhanced oil recovery (EOR) in tight oil reservoirs. Chemical Engineering Journal 452, 139454 (2023)